

UCRL- 93901 RI
PREPRINT

UCRL--93901-RI

The Compact Torus Accelerator
A Driver For ICF

DE86 014785

Michael T. Tobin
Edward C. Morse

This paper was prepared for submittal to
the 1986 ANS Annual Meeting, Reno, Nevada,
June 15-19, 1986.

July 31, 1986

This is a preprint of a paper intended for publication in a journal or proceedings. Since changes may be made before publication, this preprint is made available with the understanding that it will not be cited or reproduced without the permission of the author.

Lawrence
Livermore
National
Laboratory

DISTRIBUTION OF THIS DOCUMENT IS UNLIMITED

DISCLAIMER

This document was prepared as an account of work sponsored by an agency of the United States Government. Neither the United States Government nor the University of California nor any of their employees, makes any warranty, express or implied, or assumes any legal liability or responsibility for the accuracy, completeness, or usefulness of any information, apparatus, product, or process disclosed, or represents that its use would not infringe privately owned rights. Reference herein to any specific commercial products, process, or service by trade name, trademark, manufacturer, or otherwise, does not necessarily constitute or imply its endorsement, recommendation, or favoring by the United States Government or the University of California. The views and opinions of authors expressed herein do not necessarily state or reflect those of the United States Government or the University of California, and shall not be used for advertising or product endorsement purposes.

THE COMPACT TORUS ACCELERATOR

A DRIVER FOR ICF*

Michael T. Tobin^a
Wayne R. Meier
Lawrence Livermore National Laboratory
P. O. Box 5508, L-480
Livermore, CA 94550
(415) 423-1168

ABSTRACT

We have carried out further investigations of technical issues associated with using a compact torus (CT) accelerator as a driver for inertial confinement fusion (ICF). In a CT accelerator, a magnetically-confined, torus-shaped plasma is compressed, accelerated and focused by two concentric electrodes. Here, we evaluate an accelerator point design with a capacitor bank energy of 9.2 MJ. Modeled by a 0-D code, the system produces a xenon plasma ring with a radius of 0.73 cm, a velocity of 4×10^7 m/s, and a mass of 4.4 μ g. The plasma ring energy available for fusion is 3.8 MJ, a 40% driver efficiency. Ablation and magnetic pressures of the point design, due to CT acceleration, are analyzed. Pulsed-power switching limitations and driver cost analysis are also presented. Our studies confirm the feasibility of producing a ring to induce fusion with acceptable gain. However, some uncertainties must be resolved to establish viability.

INTRODUCTION

Using an accelerated plasma ring to compress fusion targets has distinct advantages over other drivers. The potential low cost and high efficiency would provide a significant economic advantage for a CT-driven, fusion electric power plant.

The concept is simple and may be achieved using "off the shelf" technology with certain

*Work performed under the auspices of the U.S. Department of Energy by the Lawrence Livermore National Laboratory under contract number W-7405-ENG-48.

^aSupported as a U. S. Army Military Research Associate at the Lawrence Livermore National Laboratory.

Edward C. Morse
University of California, Berkeley
Nuclear Engineering Department
Berkeley, CA 94720
(415) 642-7275

improvements in pulsed power supplies and electrode construction. We examine the conditions the electrodes must withstand for a CT with a mass and a velocity in the range required for fusion. A simple electrode design is analyzed for conductor ablation and sputtering. Further, required electrode thicknesses are determined to evaluate the electrode ability to contain the magnetic pressures. No attempt was made to optimize the design by minimizing parameters such as the CT magnetic field. We conclude that several obstacles to CT accelerator use must be overcome but that none, in itself, is insurmountable. References 1 through 3 offer a complete treatment of the topic.

THE COMPACT TORUS

The compact torus is essentially a toroidal-shaped self-contained magnetic configuration with a confined plasma. The CT structure consists of both poloidal and toroidal fields sustained by large internal currents, as shown in Figure 1.

Ring Theory and Formation/Acceleration

Taylor's Theory states that a plasma will assume the geometry of a state of minimum magnetic energy,

$$U_H = \frac{1}{2\mu_0} \int B_{CT}^2 dV_{CT} \quad , \quad (1)$$

where μ_0 is the permeability of free space, B_{CT} is the magnetic induction in the plasma ring, and integration is over the ring volume. This minimum geometry is assumed when the plasma β (ratio of thermal energy to magnetic energy) is much less than one.

A torus is the minimum volume the plasma assumes for the rail gun accelerator used here. The plasma current density, J , and

MASTER

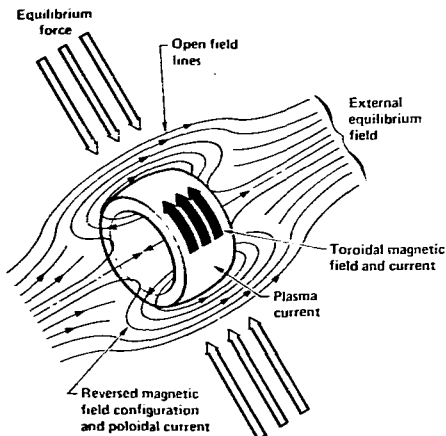


Fig. 1. The Compact Torus

magnetic induction, B , are approximately parallel, such that

$$F = J \times B = 0 \quad , \quad (2)$$

where F is the magnetic force per unit volume in the ring. Force-free currents imply a stable configuration. The ring is stable enough to undergo compression and acceleration without dissolution.

While several means exist to produce CT's, the method employed here, the co-axial rail gun, was chosen for simplicity and ready adaptation to acceleration and focusing. Here is a typical formation/acceleration sequence:² 1) The solenoid capacitor bank is fired at $t = 0$. These solenoidal magnetic field lines will become the poloidal field of the CT. 2) At $t = 1130 \mu s$, the solenoid capacitor bank is crow-barred. 3) At $t = 1180 \mu s$, the gas valve capacitor bank discharges, opening several fast puff gas valves. Gas fills the gun breech. (Figure 2a.) 4) At $t = 1580 \mu s$, the main gun capacitor bank discharges, ionizing the gas and accelerating the plasma through the toroidal field established in step one. The lines of flux collected by the plasma then become the CT poloidal magnetic field when the lines pinch off. At this point, the CT is formed. (Figure 2b,c.) 5) At $t = 1600 \mu s$, the accelerating capacitor bank is fired. The current density introduced crossed with the

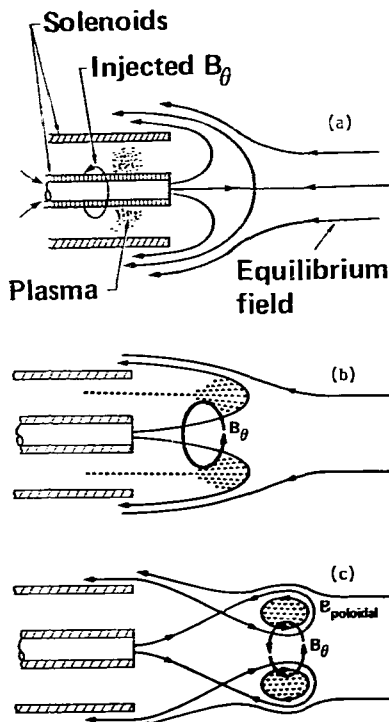


Fig. 2. Steps to CT Formation

resulting magnetic flux density produces a force that accelerates the CT. The action is similar to a magnetic piston pushing a sliding short through a co-axial pipe. 6) After acceleration, the CT is focused to the desired radius by entering a conducting cone. The compact torus now moves to interact with the fuel pellet.

CT Properties

In the ring geometry considered in this analysis, the length of the CT is equal to the ring's minor radius. Then, the poloidal and toroidal magnetic fields are approximately equal. The temperature of the compact torus, limited by oxygen and nitrogen impurities, is initially in the 10 to 40 eV range. At

formation, the torus may contain 5 kJ of magnetic energy. During acceleration, the magnetic energy decays ohmically with a time constant related by²

$$\tau = \frac{R^2 T_e}{Z_{\text{eff}}} \quad (3)$$

where R is the ring radius, T_e is the electron temperature, and Z_{eff} depicts the ionization state. During final focusing the magnetic energy increases in proportion to the inverse of the radius. The ring magnetic energy here can be 75 times the initial value, or more.

The plasma can be described as stable with experimental lifetimes exceeding 1 ms.³ However, an equilibrium force must consistently be applied to the ring to contain its magnetic fields. Without this stabilizing force, the ring's magnetic fields will expand at the Alfvén velocity.

$$v_{\text{Alfvén}} = B_{\text{CT}} (\mu_0 n_{\text{CT}} m_i)^{-0.5} \quad (4)$$

where n_{CT} is the ring ion density, m_i is the ion mass, and μ_0 is the permeability of free space. Since the ring plasma β , the ratio of thermal energy density to magnetic energy density, is small, particles adhere closely to the magnetic field lines and are well contained. Plasma leakage due to local instabilities is small.

The equilibrium force (see Fig. 1), supplied by eddy currents in the electrode walls, is removed when the ring leaves the accelerator. Since for current reactor designs, the ring must travel as much as five meters, a propagation scheme must be employed to prevent significant ring expansion before pellet interaction occurs. Two proposals by Meeker are considered.² First, a background gas in the reactor chamber would allow the ring to develop a bow-shock wave, providing a restoring force on the ring. However, this scheme would require the ring to have over 100 times more kinetic energy than magnetic energy to prevent excessive energy losses during ring transit. The accelerator examined here has a kinetic to magnetic energy ratio of only 10. Therefore, Meeker's suggestion to use lithium jets, or lithium tube that is replaced after each shot, is more feasible since the ratio of kinetic to magnetic energies is irrelevant in this scheme.

CT REQUIREMENTS FOR ICF

Design of a CT accelerator must start with identifying specific CT parameters necessary to adequately heat and compress the fusion fuel. These parameters are determined by choosing the

fusion gain, the accelerator efficiency, the CT plasma ion (Xe), and the ion range in the target. These chosen values dictate the CT velocity, mass, and final radius. In turn, the Ring Accelerator Code (RAC)⁵ determines the required specifications of the accelerator system.

Earlier, economic studies indicated that a fusion gain (ie. product of target gain and driver efficiency) in the range of 15 to 40 was desirable for a fusion electric power plant.⁶ In our CT design study, a fusion gain of 30 was chosen as a goal. Research of CT accelerator efficiency to date indicates that an efficiency of 50% is possible.⁴ However, the conservative value of 35% efficiency was selected. The required target gain was thus established as 86.

We assume 10 MJ of stored energy is available to accelerate the CT. For a repetition rate of 3 Hz and a ring with 3.5 MJ of kinetic energy, the reactor will produce 315 MWe. Later, the actual accelerator point design will have 9.2 MJ of stored energy, but produce a ring with 3.8 MJ of kinetic energy.

The interaction of the compact torus with the fuel pellet is assumed to act as a heavy ion beam with a neutral space charge. The ring's magnetic fields will be overcome by ring deceleration on impact, if ring kinetic energy is much greater than the ring magnetic energy. Rayleigh-Taylor instabilities will allow electrons and ions to cross flux lines.²

The target gain is a function of the ion range in the target. A shorter ion range generates greater target gain. We have selected the smallest range for xenon ions considered feasible for target manufacture and quality control. Xenon ions achieve a range of 0.02 g/cm² if each has 1.1 GeV of kinetic energy.⁷ The ion (and therefore ring) velocity is 4×10^7 m/s. For a ring kinetic energy of 3.5 MJ, the CT mass is 4.4 μ g.

With a range established, the CT spot size can be determined through the use of published gain curves for single shell targets.⁸ These curves are plots of target gain compared to input energy along lines of constant $r^{3/2}R$, where r is the focal spot radius (cm) and R is the target range (g/cm²). For a gain of 86, and a compact torus energy of 3.5 MJ, $r^{3/2}R$ is 0.0125. Since R has also been established as 0.02 g/cm², this indicates that the compact torus radius when reaching the target area is 0.73 cm.

The parameter space considered for the published gain curves is

$$0.1E^{1/3} < r < 0.2E^{1/3} \quad . \quad (5)$$

where E is the ring energy (MJ). The radius upper limit is 0.3 cm at 3.5 MJ. Radii larger than allowed, such as the 0.73 cm CT reduce the target gain. Although conclusive data has not yet been published, preliminary analysis indicates that a smaller radius and/or more kinetic energy may be required to achieve the gain of 86. On the other hand, more recent economic studies indicate that lower fusion gains (<10) also appear to be acceptable.¹¹

ACCELERATOR POINT DESIGN

The design of a compact torus accelerator requires extensive numerical analysis. Using the established CT mass, velocity, and final radius, we determined accelerator specifications using RAC. These values include the accelerating capacitor bank inductance, voltage, and capacitance, as well as the concentric electrode radii and overall length.

Written by B. Eddleman, RAC is a 0-D code that models CT formation, acceleration and focusing. The code models the accelerator capacitor bank and gun as a lumped LC-circuit. The circuit equation is⁴

$$L_x \frac{dI}{dt} + I \frac{dL_g}{dx} + L_g \frac{dI}{dt} = V_0 - \frac{1}{C} \int I dt \quad , \quad (6)$$

where L_x is the external inductance, I is the circuit current, L_g is the gun inductance at distance x . V_0 is the initial bank voltage, and C is the bank capacitance. The code solves this equation along with the force balance, written as

$$M_{CT} \frac{d^2x}{dt^2} = \frac{T^2}{2} \frac{dL_g}{dx} - \frac{U_M \sin \alpha}{R} - F_{drag} - F_s \quad . \quad (7)$$

where M_{CT} is the CT mass, U_M is the magnetic energy stored in the plasma ring, and R is the ring radius. The CT mass is assumed to be constant. The first term is the force on the accelerated ring. The difference between the second and third terms of Eq. 7 is the difference between the magnetic energy per unit length of the ring and the inductively stored energy per unit length behind the ring. The fourth term is a small drag force resisting ring acceleration. This drag is due to magnetic energy losses in the electrodes due to magnetic diffusion. The fifth term is the resultant force on the ring from the "sloshing" of ions within the ring during rapid acceleration and deceleration.

Magnetic and plasma energies are conserved with the appropriate balancing equations.

Our point design uses a slow compression stage for the compact torus prior to ring

acceleration. The cone shape of this design can be seen in Figure 3. The slow compression allows efficient storage of capacitor bank energy as inductively stored energy behind the ring. During slow compression, the accelerating $J \times B$ force is just balanced by the radial equilibrium force applied by the cone. The ring proceeds quite slowly until it reaches the beginning of the straight co-axial section. Here, the current and the inductively stored energy reach their maximum values. Wall image currents then provide the radial equilibrium force and the $J \times B$ force provides uninhibited acceleration.

A slow compression-type accelerator with a CT mass of 4.4 μ g was designed. Key parameters are listed in Table 1.

ELECTRODE RESPONSE TO CT ACCELERATION

An economical lifetime of the CT driver electrodes is paramount to successful reactor operation. The focusing section is exposed to ultra-high magnetic fields and potentially destructive stresses. Electrode lifetime is also shortened by sputtering when discharging at 3 Hz. Electrode design consists of two co-axial tubes of stainless steel. The inner surface of the outer electrode and the outer surface of the inner electrode are copper-plated to a depth of 0.2 cm. This design is further illustrated in Figure 3 and Table 1.

The data collected from RAC output, primarily $B_{CT}(t)$, electrode length and radius, and CT size, are ideal approximations of gun operating conditions. Therefore, results indicate only what may be possible.

Ablation

Surface wall temperatures are first analyzed to determine the location of the onset of melting or vaporization. The only significant contribution to wall heating considered was the ohmic heating caused by the diffusion of the ring magnetic field into the conductor. The conductor surface temperature due to this heating is proportional to the magnetic field squared.

The ring field diffuses on a very short time scale (ns) and to a very small depth (< 0.11 cm). Therefore, the flux density in time will be modeled as a step function, where

$$B(0,t) = 0, \text{ for } t < 0 \\ = B_0, \text{ for } t > 0 \quad . \quad (8)$$

Magnetic field diffusion into a conductor is synonymous with an influx of energy. The energy increase can be described by Joule's Law. The surface temperature reaches a maximum

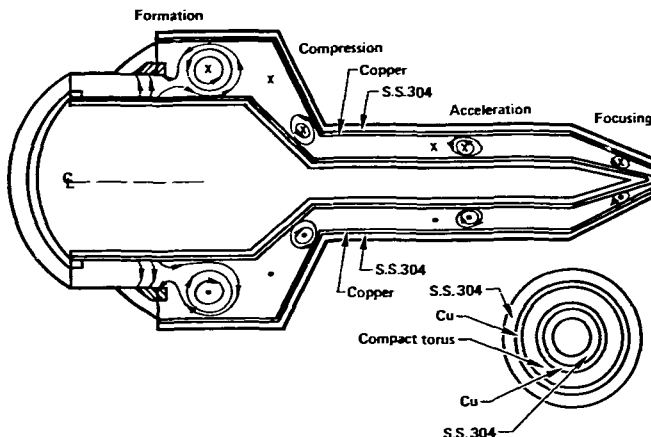


Fig. 3. Electrode Design of CT Accelerator

Table 1. CT Accelerator design parameters

CT	Capacitor Bank
Mass ~ 4.4 μgm (Xe)	Energy ~ 9.2 MJ
Final radius ~ 0.73 cm	Capacitance ~ 718 μF
Final velocity ~ 4×10^7 m/s	Inductance ~ 500 nH
Kinetic energy ~ 3.8 MJ	Voltage ~ 160 KV
Accelerator	System
Length ~ 12.3 m	Gain ~ 95
Initial radius ~ 50 cm	Efficiency ~ 41%
Current ~ 5.3 MA	Rep rate ~ 3 Hz

due to the heat conduction. For copper, this reduces to⁹

$$T_{\text{MAX}} = 5 \times 10^5 \frac{B_0^2}{C_v} \ln \left[1 + 990 \left(\frac{C_v}{k} \right)^{1/2} \right] \quad (9)$$

where B_0 is expressed in tesla, and T is expressed in $^{\circ}\text{C}$. The electrical conductivity (σ), thermal conductivity (k), and specific heat (C_v) were varied with temperature in the calculations.

The accelerator operates in a vacuum. A value of 10^{-6} atmosphere is used based on the vacuum conditions for the Beta II experiment at the Lawrence Livermore National Laboratory.⁴ The boiling point of copper (T_b) is 847°C at this pressure.

The surface and skin depth temperatures were calculated. The copper ablates approximately half-way down the final 30 cm focusing cone, where B_0 reaches 150 T. The maximum B_0 is 1588 T at the cone's tip. The volume of material ablated and vaporized with each firing was estimated to be 0.8 cm^3 . This vaporization could prevent the focusing section, over time, from maintaining the small radius rings required for the established fusion gain.

A suggested solution to this problem is to allow liquid lithium to either coat the copper or replace the copper as the conductor over the focusing length. In theory, the lithium would act as an ablator, or sacrificial surface, over the copper. However, the lithium thickness would have to be at least three times the copper skin depth to carry the same current, since lithium's resistivity is eight times greater than copper's. Maintaining a uniform film would be crucial to insuring the accelerating flux continues to evenly push the ring.

Magnetic Pressures

The same magnetic flux density that heated the conductor also subjects the gun electrodes to a magnetic stress. If the stresses are too great, the available inner electrode tip cross section may not allow for a sufficient thickness of structural material.

We assume the accelerator electrodes to be infinitely thick conductors because the ratio of the skin depth to the total conductor depth is $\ll 1$. We assume the magnetic flux density vector is everywhere parallel to the conductor surface. The resulting pressure is then everywhere normal to the conductor surface. We also assume that the conductor is non-compressible and neglect the potential formation of shock waves that could precede the ring's motion down the gun tube.

Dynamic containment of this magnetic pressure allows the inertia of the electrode to assist in resisting the resultant stress. Dynamic containment is possible because the duration of the pressure pulse (ns) is short compared to the oscillation period of the electrode(s). The criterion for dynamic containment is

$$\frac{1}{2\mu_0} \int B_0^2 dt < \left(\frac{\rho}{E} \right)^{1/2} \sigma_y d \quad . \quad (10)$$

where σ_y is the material yield stress and d is the wall thickness. The density of steel and Young's Modulus are ρ and E , respectively. The time (t) of equation 10 is the characteristic diffusion time generated by RAC. Using the surface magnetic induction for both fields (the accelerating B_0 and B_C) at several points, magnetic pressures and required steel thicknesses were calculated.

Stainless steel type 304 is used for the structural wall material, except at the inner electrode focusing cone. When the yield strength of the steel is reduced as the operating temperatures increase toward the electrode tip, a stronger material is required to meet size constraints due to the gun design. When AISI 9840 steel is used, the required wall thickness is less than the maximum allowed dimension, 0.35 cm, as shown in Figure 4. However, the steel at the tip cannot exceed an operating temperature of 500°C. Here, active cooling for the inner electrode may be significantly limited.

It is clear that the magnetic pressure, although much greater than the yield stress of steel, can be contained due to the very short exposure time. The focusing section of the accelerator may pose significant heat transfer difficulties due to limited surface area and

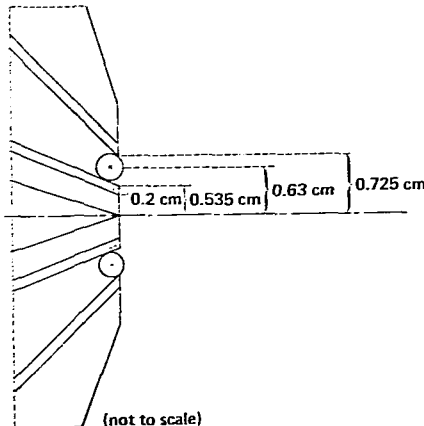


Fig. 4. Design Limitations at the Accelerator Tip

extreme conductor temperatures. Fatigue failure due to cyclic loading was not considered here.

ENERGY STORAGE/SWITCHING

The unique pulsed power supply for the accelerator will be expected to outperform any very large power system available today. The system must transfer very large currents at a very high voltage in a very short time period. The only technology currently available with the very short rise time required (10 to 20 μ sec) is the capacitor bank system, excluding fast high explosives.

Switching Limitations

A limiting factor for today's fast-closing switches is the inability to discharge at a very fast repetition rate, at the required high voltages and currents, over an extended time period.

Magnetic switching may provide a reliable means to transfer large currents at high voltages with a high repetition rate. The principle behind magnetic switching is to use the large changes in permeability exhibited by saturating ferri- (ferro-) magnetic materials to produce large changes in impedance. Initially at high-impedance (large permeability) the material, as an inductor, performs like an open switch. At peak voltage, the material saturates and the inductor attains

a low-impedance (small permeability). The switch is then closed. The quantity of material required depends on the peak voltage applied and the input pulse width ($\int Vdt$). While large voltage-pulse width products imply large amounts of material, this material does not experience the stresses of conventional spark gap switch materials and therefore may have an extremely long lifetime.¹⁰

COST

A simple cost analysis was performed to confirm preliminary estimates that this driver could deliver energy at a cost on the order of dollars per joule. The accelerator capacitor bank is by far the most expensive single component. The cost of the entire compact torus accelerator system is virtually this bank's cost plus a few percent. Results indicate that the CT may deliver energy at a cost of \$10/J, assuming 35% efficiency. This figure represents a preliminary estimate and is meant to serve as a start point for future more detailed design/cost analysis. This driver coupled with the Cascade reactor cost results in a cost of electricity (COE) of about 3¢/KWh. This is 10 to 20% less than the estimated COE with a laser driver at \$100/J (direct) and nearly 50% less than the estimated COE using a heavy ion beam driver.¹¹

CONCLUSION

A viable electrode design for a CT accelerator must include a sacrificial lining/conductor along part of the focusing cone, or some means to counter the intense inductive heating. The driver heat transfer system must remove heat fast enough to support the reactor repetition rate. Also, this system must maintain the electrode load bearing materials (like steel) at a temperature that avoids significant reduction in yield strength to contain the magnetic pressure.

Using the CT accelerator as a driver for ICF is exciting and full of potential. If experimental efforts at confirming acceleration and focusing are successful at LLNL in the next few years, attention will be drawn to the CT from many disciplines. As the many diverse applications for the CT are explored, collaboration on difficulties for the ICF application is inevitable and should receive broad based attention.

REFERENCES

1. M. T. TOBIN, Investigation of the Compact Torus as a Driver for Inertial Confinement Fusion, Master's Thesis, University of California, Berkeley(1985).
2. D. J. MEEKER, "A High Efficiency ICF Driver Employing Magnetically Confined Plasma Rings", Fusion Technology, 8, 1-2B(1985).
3. T. R. JARBOE, et al., Proc. Sixth Symposium Phys. Technol. Compact Toroids, Princeton Plasma Physics Lab, Princeton, NJ, (1984).
4. C.W. HARTMAN and J. H. HAMMER, Acceleration of a Compact Torus Plasma Ring, A Proposed Experimental Study, LLL-PROP-191, Lawrence Livermore National Laboratory(1984).
5. J. EODLEMAN, Ring Accelerator Code, Lawrence Livermore National Laboratory(1980).
6. M.J. MOWSLER et al., "An Overview of Inertial Fusion Reactor Design", Nuclear Technology/Fusion, 1, 302(1981).
7. R. BANGERTER, "Heavy Ion Inertial Fusion: Initial Survey of Target Gain Versus Ion-Beam Parameters", Physics Letters, 88A, 5 (1982) and private conversation.
8. J.W.K. MARK, Recent U.S. Target Physics Related Research in Heavy-Ion Inertial Fusion: Target Gains and Relation to Accelerator Design, UCRL-87378, Lawrence Livermore National Laboratory(1982).
9. H. KNOEPFEL, Pulsed High Magnetic Fields, North Holland Publishing Company, Amsterdam(1970).
10. D. BIRX, et al., "Magnetic Switching" Final Chapter Book I: The ATA Upgrade Prototype, UCRL-89128, Lawrence Livermore National Laboratory(1983).
11. H.R. MEIER, H.J. HOGAN, and R.O. BANGERTER, "Economic Studies of Heavy Ion Fusion Electric Power Plants", UCRL-94335, Lawrence Livermore National Laboratory(1986).